Importance of parental genome balance in the generation of novel yet heritable epigenetic and transcriptional states during doubled haploid breeding

Jonathan Price[1], Javier Antunez-Sanchez[1], Nosheen Hussain[1], Anjar Wibowo[2, 3], Ranjith Papareddy[1, 4], Claude Becker[2, 4], Graham Teakle[1], Guy Barker[1], Detlef Weigel[2] and Jose Gutierrez-Marcos[1]

[1] School of Life Sciences, University of Warwick, Coventry CV4 7AL, UK
[2] Department of Molecular Biology, Max Planck Institute for Developmental Biology, Tubingen, Germany
[3]Faculty of Science and Technology, Airlangga University, Kampus C, Mulyorejo, Surabaya City, East Java 60115, Indonesia
[4]Gregor Mendel Institute of Molecular Plant Biology, Austrian Academy of Sciences, Vienna Biocenter (VBC), 1030 Vienna, Austria

To whom correspondence should be addressed. Email: j.f.gutierrez-marcos@warwick.ac.uk

Keywords: Genome merger, breeding, epimutation, transposon

Abstract

Background: Doubling the genome contribution of haploid plants has accelerated breeding in most cultivated crop species. Although plant doubled haploids are isogenic in nature, they frequently display unpredictable phenotypes, thus limiting the potential of this technology. Therefore, being able to predict the factors implicated in this phenotypic variability could accelerate the generation of desirable genomic combinations and ultimately plant breeding.

Results: We use computational analysis to assess the transcriptional and epigenetic dynamics taking place during doubled haploids generation in the genome of *Brassica oleracea*. We observe that doubled haploid lines display unexpected levels of transcriptional and epigenetic variation, and that this variation is largely due to imbalanced contribution of parental genomes. We reveal that epigenetic modification of transposon-related sequences during DH breeding contributes to the generation of unpredictable yet heritable transcriptional states. Targeted epigenetic manipulation of these elements using dCas9-hsTET3 confirms their role in transcriptional regulation. We have uncovered a hitherto unknown role for parental genome balance in the transcriptional and epigenetic stability of doubled haploids.

Conclusions: This is the first study that demonstrates the importance of parental genome balance in the transcriptional and epigenetic stability of doubled haploids, thus enabling predictive models to improve doubled haploid-assisted plant breeding.

Keywords: Genome balance, plant breeding, doubled haploid, genome merger, DNA methylation, genome dosage.

Background

Most organisms require genetic information that is inherited from both parents; however, plants have the unique capacity to generate viable haploid offspring [1]. Haploid plants can originate spontaneously in nature, through parthenogenesis or chromosome elimination, usually associated with interspecific hybridization. Plant haploids can also be induced *in vitro* by culturing female and male plant gametophytes [2]. Doubling the genomic contribution of plant haploids, spontaneously and through human intervention, led to the discovery of doubled haploids (DHs) [3]. DHs allows the generation of homozygous individuals in one generation, reducing the number of cycles necessary for the selection of qualitative and quantitative characters and thus accelerating plant breeding [4, 5]. DH breeding is particularly advantageous in species that display barriers to repeated selfing, such as dioecy and self-incompatibility, or having long juvenile periods [6]. The production of DHs is only available to a limited number of plant species and defined genotypes, with protocols often having a low embryo yield, therefore most studies have centred on the development of efficient haploid induction protocols [5]. Standard DH breeding schemes start with the crossing of desirable genotypes, leading to hybrids containing chromosome sets from both parents. During gamete formation, recombination enables the formation of new genomic combinations, which can be fixed during doubled haploid induction. However, although DHs are isogenic in nature, they frequently display unpredictable phenotypes, thus limiting the efficacy of this technology in plant breeding [7]. The combination of two diverged plant genomes in hybrids and allopolyploids also result in unstable phenotypes that differ from both parents, which have been attributed to transcriptional variation underpinned by the genomic and epigenomic differences of the parents [8-13]. The precise origin of this transcriptional variation remains largely unknown; however, recent studies in plants have implicated small interfering RNAs (siRNAs) and RNA-directed DNA methylation (RdDM) as main contributors [14].

In this study, we investigated the transcriptional and epigenetic dynamics associated with DH production in *Brassica oleracea*. We found that the transcriptional instability present in DHs is largely caused by the imbalanced contribution of paternal genomes. Moreover, we demonstrated that this transcriptional variation is associated with changes in DNA methylation, primarily at transposon (TE)-related sequences, which is created during genome merging in DHs.

Results

Transcriptional and epigenetic changes in *B. oleracea* parental lines and hybrids

To uncover the transcriptional dynamics at play in DHs, it is important to understand first the gene expression differences between parents and hybrids. Our data show 3,216 parental differentially expressed genes (pDEGs), which accounts for 6.2% of the genes annotated in the *B. oleracea* genome, with no bias for under- / over-expression in either parental line (Figure S2). Gene Ontology (GO) enrichment analysis revealed that pDEGs are over-represented for genes implicated in transcription and translation (Table 1). When we performed comparisons between parents and F1 hybrids, we found 3,353 parent-hybrid differentially expressed genes (phDEGs), however only 137 phDEGs were not identified as pDEGs (Figure 1a). The expression of these phDEGs in the F1 hybrid can be explained in terms of their dominance-to-additive expression relationship (Figure 1b). A large proportion of phDEGs (2,234/66.6%) displayed additive expression in F1 hybrids when a smaller fraction (1,110/33.3%) displayed non-additive or unexpected expression patterns (Figure 1b). The majority of the non-additively expressed phDEGs showed expression level dominance (most similar to one of the parents), yet a small number of phDEGS (200) showed transgressive expression (outside parental range). We found that there was a large bias in the non-additively expressed phDEGs for A12DHd expression level dominance (843 out of 1,119). This bias was independent of the direction of the difference in the parents and followed the expression of the A12DHd parent independently of GDDH33 expression (Figure 1b,c). This finding was also supported by the clustering of the F1 for both additive and non-additive phDEGs with A12DHd (Figure S3).

The transcriptional changes taking place in F1 plant hybrids have been attributed in part to epigenomic changes present in the inherited parental genomes [9]. We therefore investigated the genome-wide changes in DNA methylation in founding parents and hybrids. As reported for other plant species, the distribution of DNA methylation in these samples was different for each sequence context (Figure S4a). At the chromosome level, DNA methylation accumulated at peri-centromeric regions and in particular within transposons. Our data show that rate of methylation at symmetric sites (CG and CHG) was higher in A12DHd, in particular at genic regions, and that in the F1 hybrid methylation operated at a mid-parent value. However, asymmetric methylation (CHH) was higher in GDDH33, specifically at transposon sequences, and reduced in F1 hybrids (Figure S4). Because there is little evidence supporting single-cytosine-methylation differences associated with gene expression changes, we focused our analysis in the identification of differentially methylated regions (DMRs). We found a large number of DMRs between parents (22,021 CG, 8,905 CHG and 13,009 CHH), which we defined as parental differentially methylated regions (pDMRs). Consistent with the distribution of methylated cytosines, most symmetric pDMRs were hypermethylated in A12DHd, however most asymmetric pDMRs were hypermethylated in GDDH33 and associated with transposon-related sequences (Figure S5). We then looked for methylation differences between parent

and hybrids (phDMRs) and found that most CG-phDMRs (23,264, 95%) are already present in the parents. In contrast, non-CG phDMRs in the F1 hybrid were novel and not always present in parental genomes (CHG 3719-29%, CHH 9041-41%) (Figure 2a). To better understand the methylation interactions occurring in the hybrid, we determined their dominance-to-additive relationships (Figure 2b). We found that CG-phDMRs were mostly additive (63.5%) and located in genic region, however non-CG phDMRs displayed lower additive interactions (37.3% at CHG-phDMRs and 20.3% at CHH-phDMRs). For non-additive phDMRs, the methylation of these regions resembled the A12DHd parent (CG-phDMRs 6144/7649, 80%; CHG-phDMRs 2,642/4,360, 60%; and CHH-phDMRs 5,895/8,281, 71.1%). Most of the non-additive CG-phDMRs were associated with trans-chromosomal methylation events (TCM), while non-CG phDMRs were primarily associated with trans-chromosomal demethylation (TCdM) (Figure 2bc and Figure S6). However, even considering the large proportion of A12DHd dominant hypomethylation at CHH-phDMRs (71%) we found that F1 hybrids accumulated widespread transgressive hypomethylation primarily at intergenic regions of the genome (Figure 2). When we looked at the methylation profile of TEs, we found that methylation at CG and CHG sites were almost identical for parents and hybrids; however, methylation at CHH sites differed, with GDDH33 showing higher methylation levels across most TE families and F1 hybrid methylation similar to A12DHd parent (Figure S4). Taken together, both expression and methylation in the F1 hybrid showed an imbalance toward the A12Dhd parent.

Transcriptional changes in *B.oleracea* DH lines

Plant DHs have been associated with unpredictable yet stable phenotypes, which can be selected/fixed by conventional breeding [15-17]. To determine the mechanisms underpinning these effects, we conducted a genome-wide analysis in nine DH lines (Figure 3). We determined the precise parental genome contribution of each DH line using epi/genetic genotyping (See Methods and Figure S8 and S9). We identified 320,339 single nucleotide polymorphisms (SNPs) and 228,642 epigenetic variants that could distinguish each parental genome. Using these markers, we determine the location of homologous recombination (HR) breakpoints with an average resolution of 130 kbp (2.3–807kbp. Our data showed a distribution of 0.88 HR sites per chromosome per DH line (Figure 3), which is concordant with other studies in related species [18, 19]. Using this information, we divided the transcriptome data for each DH line according to parental genome inheritance and performed pairwise comparisons to identify genes that were differentially expressed between the DH line and the relevant parent. Our analysis identified 1,820 dhDEGs, ranging from 156-736 genes per DH, which accounts for 0.3 - 1.4% of the transcriptome. Notably, a large fraction of genes that showed additive expression in hybrids reset their expression to normal parental levels in DHs

(Figure 4a,b) (X^2 (df = 4, N =3254) = 145.7, p-value <0.001). However, some genes differentially expressed in DHs already showed differences in parental expression in F1 hybrids (Figure 4a,b). Markedly, the majority of these dhDEGs, and in particular those inherited from GDDH33, displayed expression-level dominance (Figure 4b and Figure S10). Our data suggest that the regulatory components implicated in DH gene expression are more complex than previously anticipated. One component that may be important for gene expression level dominance in DHs is the proportion of parental genome created. To test this hypothesis, we looked for a correlation between gene expression change and parental genome inheritance. Our data show a significant negative relationship between transcriptional perturbation and imbalanced parental genome contribution (Figure 4d). Notably, DH lines inheriting an imbalanced proportion of parental genomes could experience up to three times more changes in gene expression than lines inheriting a balanced parental genome contribution (Figure 4d and table 4). Gene ontology analysis revealed that genes implicated in response to environmental stimuli were particularly enriched (Figure S11). Because DH lines from distant parents have an isogenic yet mosaic genomic structure, regulatory elements needed for proper transcription may be imbalanced.

Epigenetic changes in *B.oleracea* DH lines

To determine if these transcriptional changes in DHs are associated with epigenetic variation, we performed a whole-genome methylome analysis using plants originating from DHs propagated by self-fertilisation over two consecutive generations. Our data shows that all DH lines accumulated significant differences in DNA methylation (dhDMRs) when compared to their inherited parental genomes (ranging from 1,911-6,431 at CG-context; 3,771-9,430 at CHG-context; 5,224-12,021 at CHH-context) (Figure 5a). We then compared the methylation dynamics at dhDMRs with that of hybrids (phDMRs) and found that most of these changes occurred at non-CG dhDMRs. Some of this differential methylation was already present in F1 hybrids, thus suggesting that this epigenetic variation was not reset during meiosis, haploid production and chromosome doubling, and that this variation was stably inherited over multiple generations. These dhDMRs were both hypo- and hyper-methylated, affected equally both parental genomes and were primarily associated (>70%) with transposons at intergenic sequences (Figure 5a,b). Notably, these non-CG dhDMRs displayed parental methylation dominance and have a significant association with the methylation status detected in hybrids (Figure 5c) (CHG = X^2 (df = 4, N = 11,946) = 483.6, p-value <0.001); CHH = X^2 (df = 4, N = 20,199) = 2,509.5, p-value <0.001). On the other hand, CG-dhDMRs were five-fold less abundant in DHs than in hybrids, indicating that these genome regions displayed a tendency (>70%) to reset their methylation to parental levels in DHs. When we looked at the methylation dynamics of these DMRs, our data showed that regions inherited from GDDH33 were more

resistant to reset their methylation to parental levels (T-test, t=-2.224, p-value= 0.0485). Moreover, these GDDH33-dhDMRs were primarily hypomethylated, located near genes, and their methylation status inherited over multiple generations (Figure 5 a, c). Our data also show that transposons in DHs were methylated at mid-parent values at CG sites but displayed transgressive values at non-CG sites (Figure S12). When we looked at the methylation of different transposon types, we found that those inherited from GDDH33 displayed greater differences in methylation than those inherited by A12DHd (Figure S12). We then analysed the relationship between parental genome dosage and epigenetic change, as this factor was a major feature associated with transcriptional perturbations in DHs. CG-dhDMRs were affected by the proportion of parental genomes inherited (A12DHd r^2=0.68, FDR,0.01; GDDH33 r^2=0.40, FDR<0.01). Low contributions from either parent (>20%) in a DH line could be associated with up to 3-fold change in methylation on those inherited regions (Figure 5d and Figure 4). Our data also revealed that half of the differential methylation in DHs at CG sites occurred within genes or nearby flanking regions (Figure S13). This epigenetic variation has the potential to be associated with changes in gene expression, thus to test this hypothesis we looked for dhDMRs that may explain the behaviour of the identified dhDEGs. Our data showed that dhDMRs occupied 4.7% of the *B. oleracea* genome (Figure 6a), of which 0.4% were located in proximity to annotated genes. We reasoned that if dhDMRs have a conserved regulatory function, they would display a correlation between methylation status and gene expression in all DH lines and stable over generations. We identified 247 genes that showed a significant correlation (FDR<0.01, Table 5), most of them had an assigned function, five were annotated as retrotransposons and forty were of unknown function. We then investigated each intersected genomic region (see methods) and selected a small subset for detailed analysis (Figure 6c and Figure S14). We selected one of these candidate dhDMRs because it was associated with intragenic retrotransposon-like copia (RLC) sequence and located within an AGAMOUS-like gene (Bo6g014360) (Figure 6c). In parental lines, this RLC was differentially methylated at symmetric cytosine sites and the methylation status of this dhDMR was directly correlated with Bo6g014360 expression. Notably, in F1 hybrids both DNA methylation and gene expression displayed mid parent values. However, DH lines that inherited this genomic region from the A12DHd parent displayed variable methylation patterns. These epigenetic imprints were heritable over multiple generations and showed a strict correlated with defined transcriptional states (Figure 6d). This transgressive methylation most likely occurred in the hybrid or during doubled haploid induction, and the newly formed epigenetic/transcriptional state was meiotically inherited over multiple generations. To demonstrate the hypothesis that methylation act as a transcriptional regulatory module, we employed a targeted demethylation approach using DH2069, which displayed hypermethylation of RLC and low Bo6014360 expression (see methods). We found that the

231 depletion of RLC methylation resulted in a noticeable increase in Bo6014360 expression
232 (Figure 6 d, e). Collectively, our data show that the stochastic transcriptional variation present
233 in plant DHs originates from epigenetic changes created at discrete genomic regions during
234 doubled haploid induction and that are heritable to offspring.
235
236 **Discussion**
237 The combination of divergent genomes, both in animals and plants, can result in unexpected
238 transcriptional and epigenetic variation [20, 21] and their study has led to insights into genome
239 regulation, breeding and evolution [13, 22, 23]. However, these studies have been primarily
240 focussed on the genome mergers of hybrids and polyploids [8]. The conventional view is that
241 the creation of transcriptional and epigenetic perturbations in genome mergers is largely
242 caused by the evolutionary distance between parents [8, 9]. We have found that *B. oleracea*
243 hybrids also show unexpected transcriptional and epigenetic variation, which can be inferred
244 from parental transcriptional variation. Most of the variation present in hybrids reverted to
245 parental levels in genetically isogenic DHs, thus suggesting that attenuation of the hybrid
246 genome shock is achieved by chromosome doubling in haploid plants as it has been observed
247 in plant allopolyploids [24]. However, our data also show that some of the perturbations in
248 gene expression and DNA methylation present in hybrids were not fully reset in DHs and in
249 particular affecting one of the parental genomes. Most of the loci displaying transcriptional
250 perturbations in DHs displayed expression-level dominance (ELD)- an effect usually found in
251 hybrids and allopolyploids [10, 21, 25, 26]. ELD effects in DHs were not only observed at the
252 transcriptional level but were also noticeable at differentially methylated CG sites near genic
253 regions of the genome. Dynamic methylation changes near genic regions have been reported
254 for other genome mergers and have been attributed to the spreading of methylation from
255 transposons unequally contributed from each parent [8]. Our data show that the molecular
256 perturbations observed in DHs are also caused by differences in parental genome size. This
257 parental imbalance could result in a mismatch in the affinity of regulatory factors [27, 28];
258 however, the DH parents we employed are nearly identical at the genome level. The
259 epigenetic variability observed in *B. oleracea* hybrids could be associated with the imbalanced
260 contribution of non-coding small interfering RNAs (siRNAs), which primarily originate from
261 transposon-like sequences and are known to direct methylation changes through the RNA
262 directed DNA methylation (RdDM) pathway [29]. Our data shows limited correlation between
263 gene expression changes and DNA methylation variation in DHs, but we found genes
264 regulated by differential methylation, which we confirmed by targeted demethylation.
265 Molecular assisted breeding using DHs in plants is commonly used to accelerate the selection
266 of desirable phenotypes; however, this methodology is costly and sometimes not fully
267 predictable [7]. Therefore, the ability to predict the molecular stability of DHs is critical to

streamline current practices. Our data reveals three factors implicated in the molecular stability of DHs: perturbations originated in hybrids that are transmitted to DHs, dominance effects, and parental genome balance. Our data show that the perturbations originated in hybrids have the smallest effects in DHs and that they could be predicted from the differences already existing in the parents, as it is the case for hybrids created from genetically distant parents [9]. Morevoer, parental dominance is another good predictor for molecular perturbations in DHs. Parental dominance is a phenomenon known to occur frequently in hybrids from plants [30] and animals [31, 32]. Although the precise molecular mechanisms underpinning parental dominance in hybrids remain largely unknown [28], it is thought to form the basis of hybrid vigour [33, 34]. Notably, our data revealed that unbalanced contribution of parental genomes in DHs was a very strong predictor of molecular change, a factor that it is not usually included in genetic selection programs using DHs [35].

Our data show the molecular variation present in plant DHs during doubled haploid induction, and that this variation could be inherited to offspring, thus it provides a platform for artificial selection to increase the yield potential of crops [15-17]. Considering the importance of DHs in plant breeding, future studies using DH populations with different parental genome contributions and grown under different experimental conditions will be needed to understand the impact of gene-environment interactions in DH-assisted breeding.

Conclusions

Doubling the genome contribution of haploid plants to create isogenic lines has been a critical component of modern plant breeding. Despite the significance of this technology, little is known of the molecular changes occurring during DH production. The approaches and findings described here provide insightful clues for future research on the prediction of phenotypic stability in doubled haploids that will enable the generation of targeted genomic combinations to accelerate DH-assisted breeding.

Acknowledgments: We thank C. Lanz and J. Hildebrandt for help with Illumina sequencing; Supported by ERC AdG IMMUNEMESIS, DFG SPP1529 and Max Planck Society to D.W., and BBSRC grants (BB/N00194X/1, BB/P02601X/1 and BB/S020934/1) to J.G-M.

Author contribution: J.P. and JG-M conceived the project. J.P, N.H, A.W., R.P., C.B. designed and conducted experiments. G.T. provided plant accessions. J.P, J.A., N.H. and JG-M analysed the data. J.P. and JG-M wrote the manuscript with input from the rest of the authors.

Declaration of interest: The authors declare that they have no competing interests.

Data and Materials Availability: Sequence data (BS-seq and mRNA-seq) that support the findings of this study have been deposited at the European Nucleotide Archive (ENA) under the accession code ERP112441.

Methods

Plant materials and growth conditions

For this study we employed a Brassica oleracea doubled haploid (DH) population initiated by Bohuon EJ, Keith DJ, Parkin IA, Sharpe AG and Lydiate DJ [36]. This DH population was generated via microspore culture using two polymorphic DH parents *B.oleracea ssp. italica* (GDDH33: D.J. Keith, John Innes Centre, Norwich) and *B.oleracea ssp. alboglabra* (A12DHd: D.J. Keith, John Innes Centre, Norwich). Parents were cross-pollinated to create a set of identical F1 hybrids from where immature microspores were collected and subjected to culture. Haploid plants generated by microspore culture were treated with colchicine and DH were propagated by selfing. We selected nine DH lines based on their genome contribution and propagated them for three generations (Fig S1).

RNA-seq processing and alignment

Total RNA-Seq was extracted from the six leaf of five plants and libraries were created using the Illumina TruSeq Stranded total RNA. These libraries were sequenced as 150bp reads on an Illumina HiSeq 4000, sequence data was assessed for quality using FastQC [37] and low quality reads were trimmed using Trimmomatic [38] (Parameters;(ILLUMINACLIP:2:40:15),(LEADING:30),(SLIDINGWINDOW:4:20),(MINLEN:36). SortmeRNA (Kopylova et al., 2012) was then used to remove remaining rRNA contamination and reads were then aligned to *Brassica oleracea* TO1000DH reference genome [39] using Tophat 2 [40]. Raw gene counts were obtained from the Python package htSeq-count [41]. Differential gene expression was analysed using DESeq2 [42] and gene was considered differentially expressed if it experienced a fold change > 1 and an FDR-corrected p-value < 0.05.

Bisulphite sequence processing alignment and calling DMRs

Genomic DNA was extracted from leaf material using the DNAeasy Plant Kit (Qiagen) and libraries were created using the Illumina TruSeq Nano Kit (Illumina, CA) according to manufacturer's instructions. After adapter ligation, DNA was treated with sodium bisulfite using the Epitect Plus kit (Qiagen, Hilden, Germany) as decribed previously (Wibowo et al., 2016). Reads were first assessed for quality using FastQC and then trimmed for low quality sequences using Trimmomatic [38]. Bismark [43] (options (-n 2, -l 28)) was used to align all

reads to the *Brassica oleracea* TO1000DH reference genome [39]. Duplicates were removed using GATK and then -CX report files were generated using Bismark. Statistics from single cytosine methylation were parsed from these files and they are also the substrate for calling differentially methylated regions (DMRs).

Differentially Methylated regions

Differentially Methylated regions (DMRs) were called using DMRCaller [44]. To allow direct comparison of regions in different comparisons the bin method was performed. To account for the different distributions of the three cytosine contexts, the required methylation difference was calculated for each sequence context (CG = 0.6, CHG = 0.35, CHH = 0.2) other parameters were (Bin size = 100, minCyt = 4, minReads = 4, minGap = 150, pValueThreshold = 0.01).

Parent-hybrid differential expression and methylation

Differences in DNA methylation and gene expression were called pairwise between the three parent and hybrid genotypes. The dominance effects on differentially expressed genes (DEGs) in the hybrid was assessed using dominant-to-additive (d/a) ratios [45]. The expression ratios of the hybrid was defined according to the A12DHd or GDDH33 parent (Figure S7) thus allowing the clustering of phDEGs into twelve mutually exclusive possible categories.

Homologous Recombination site detection

To generate the most accurate view of the crossover landscape in DH lines we combined SNP genotyping and epigenotyping. First, we developed a pipeline that utilises bisulphite data to identify polymorphic sites [46]. We generated custom scripts that first identify homozygous positions in the parental lines that differ in their base call and then looks for the parental genotype in the DH lines. For epi-genotyping we used an stablished pipeline [47] with a few modifications; we used only CG methylation, we used altered class weights (Mother-0.5, Mid-parent value-0, Father-0.5) and lastly we used bin sizes of 150kb, 70kb and 60kb. In 94% of cases the SNP and epigenetic markers agreed with the placement of the HR site and at these sites the smallest undetermined region was used. In cases where the two methods did not agree (<5 HR sites) they were manually investigated.

Gene expression and DNA methylation dynamics in DH lines

To determine the changes in gene expression and DNA methylation we used HR data to generate parent genome maps for each DH line. We then performed comparisons between parental and DH genome regions. Molecular changes in these genome segments were

379 determined as the percentage of genome inherited / number of DMRs or DEGs and their
380 relationship was determined by linear regression using these values.
381
382 **Intersection between different genomic features**
383 To determine the interaction between different genomic features we used a hierarchical
384 method to account for potential overlap (gene, transposon, upstream, downstream, intergenic;
385 in order of decreasing importance). We developed a customised script
386 (https://github.com/PriceJon/GFF_Intersector) to intersect all coordinates and performed a
387 Spearmans Rank correlation analysis to assess the strength of the relationship (FDR < 0.01).
388
389 **Targeted demethylation of genome regions**
390 We generated plasmid containing the catalytically inactive SpCas9 fused to the catalytic
391 domain of the humanTET3 (aa 850- 1795) by PCR amplification. We subcloned the dCas9-
392 TET3-CD fragment into a plasmid containing the Arabidopsis Ubiquin-10 (AtUbi10) promoter
393 using Gateway recombination. We designed four sgRNAs targeting the methylation region
394 detected in Bo6g014360 that were subcloned into a plasmid containing the Arabidopsis U6
395 (AtU6) promoter. We transfected different plasmid combinations in *Brassica oleracea*
396 protoplasts using PEG-calcium transfection [48]. Transfected protoplasts were incubated in
397 the dark at 22C for 48 hours.
398
399 **McrBC PCR analysis**
400 DNA was extracted using DNeasy Plant Mini Kit (Qiagen) and measured the concentration
401 using a Qbit fluorometer. 500 ng of DNA at 20 ng/ml was incubated with 20 U McrBC (New
402 England Biolabs) for 4h at 37C followed by heat inactivation at 80C for 15 min. Target regions
403 were amplified by PCR from 20-ng digested DNA using primers described in Supplementary
404 Table S7.
405
406 **RT-PCR expression analysis**
407 RNA was extracted with RNeasy Plant Mini kit (Qiagen) and cDNA synthesis was performed
408 as per the manufacturer's protocol using random hexamers (Superscript III, Invitrogen). Semi-
409 quantitative PCR was performed using primers described in Supplementary Table S7.
410
411
412 **Figure legends -main**

413 **Figure 1. Gene expression dynamics in the *B. oleracea* F1 hybrids. a)** Venn diagram
414 showing parental DEGs (blue) from the comparison between A12DHd and GDDH33, and the

parental and hybrid DEGs (brown) from all 3 comparisons (A12DHd - F1, GDDH33 - F1 and A12DHd - GDDH33). This plot shows there is little novel differential expression in the F1 hybrid. b) Dominant-to-additive plot showing expression dynamic of phDEGs in the F1 hybrid relative to the parental expression. Each phDEGs ratios are plotted, the d/a ratio on the y-axis and the parental d/a ratio is plotted on the x-axis. Plotting in this way, each phDEG can be categorised according to both the high / low parent and the maternal/paternal parent as shown by the numbers in the quadrants of the graph. c) Shows the categorisation of each gene. Roman numerals show the categories as they are commonly described (Yoo et al., 2013). Underneath the Roman numerals in the table, there is a graphic displaying the expression or methylation pattern of this category for the 3 genotypes (A12DHd - maternal, GDDH33 - paternal and F1) then underneath that are the proportions of the phDEGs belonging to 12 mutually exclusive expression patterns.

Figure 2. Methylation dynamics in *B. oleracea* F1 hybrids. a) Venn diagram and barchart b) Dominant-to-additive plots showing methylation dynamics of phDMRs in F1 hybrid relative to the parental methylation. Each phDMRs ratios are plotted, the d/a ratio on the y-axis and the parental d/a ratio is plotted on the x-axis. Plotting in this way, each phDMR can be categorised according to both the high/low parent and the maternal/paternal parent as shown by the numbers in the quadrants of the graph. This shows the categorisation of each phDMR. Roman numerals show the categories as described by Yoo MJ, Szadkowski E and Wendel JF [21]. Graphic display under Roman numerals display the expression or methylation pattern of this category for the 3 genotypes (A12DHd - maternal, GDDH33 - paternal and F1) and the proportion of phDMRs belonging to 12 mutually exclusive expression patterns in each sequence context.

Figure 3. Parental genome contribution of *B. oleracea* DH lines. a) Proportion of both parental genomes inherited in nine DH lines. b) Circos plot displaying the chromosome structure of each DH line.

Figure 4. Expression dynamics in *B. oleracea* DHs. a) Venn diagram showing the phDEGs (brown) and the DEGs identified from the DH lines in generation 1 split by the parent from which they were inherited. b) Bar chart showing the F1 expression dynamics of the dhDEGs (A = A12DHdh dhDEG and phDEG, G = GDDH33 dhDEG and phDEG, R = dhDEG but not phDEG). There is a significant association between the category of DEG and the expression in the F1 (X^2 – (df = 4, N = 3254), p-value < 0.001) . c) There are more dhDEGs on GDDH33 inherited genomes than A12DHd (T-test – (t = -2.047, p-value = 0.03174)). d) Relationship between percentage inheritance of parental genome and relative gene expression change

(The number of genes per DEG inherited) in DH lines. The significant relationship via linear regression are shown as lines.

Figure 5. Methylation dynamics in *B. oleracea* double haploids. a) Venn diagram with the parental and hybrid DMRs identified in Chapter 4 and the dhDMRs from each line, split by parental inheritance and their overlapping DMRs. b) Shows the F1 expression dy- namics of the phDMRs that overlap with dhDMRs (A = phDMRs and A12DHd inherited dhDMRs, G = phDMRs and GDDH33 inherited dhDMRs) and the phDMRs that recover in the DH lines (R) these are sections shown in the venn diagrams in panel a. There is a significant association between F1 methylation dynamics and the category of DMR (CG = X2 (df = 4, N = 22807) = 465.5, p-value <0.001), (CHG = X2 (df = 4, N = 11946) = 483.6, p-value <0.001), (CHH = X2 (df=4,N=20199)=2509.5,p-value<0.001). c) There are more CG dhDMRs on A12DHd in- herited genome sections than GDDH33 genome sections (CG - T-test (t = -2.224, p-value = 0.0485)). CHG and CHH inherited sections do not show significant differences (CHG - (t = 0.601, p-value = 0.5583), CHH-(t=0.743, p value=0.4689)). d) For each inherited genome in each DH line the relative gene methylation change (dhDMRs per MR inherited) is plotted against the amount of genome inherited from that parent. The significant relationships are shown as lines calculated by linear regression. Non-significant relationships are shown as a faint line.

Figure 6. Intersection of DMRs and Genomic features in *B. oleracea* DHs. a) Venn diagram showing extent of DMR and gene overlap in base pairs. b) The three DMR contexts have different distributions across the genes and flanking regions with which they overlap. Density plot showing the distribution of dhDMRs in each sequence context across the genes they overlap with. c) Example of the most highly correlated expression and methylation for a gene, *AGAMOUS-LIKE* (Bo6g014360). Left side of the plot shows a single nucleotide resolution plot of methylation across the region, the right side of the plot shows gene expression. d) McrBC assay showing the targeted removal of DNA methylation at the Bo6g014360-DMR using dCas9-TET3CD. e) RT-PCR assay showing an enhancement in Bo6g014360 transcription upon removal of DNA methylation using dCas9-TET3CD.

Figure legends - Supplementary

Figure S1. Schematic diagram of breeding scheme for samples used in this study. Each sample consists of two bars representing their diploid genome structure (yellow - A12DHd, blue – GDDH33). Samples from G1 and G3 were used for RNA sequencing and bisulphite

485 sequencing analysis. Arrows indicate the methods of generation of each sample in the
486 breeding program. Line numbers of the DH lines are shown below each line.
487
488 **Figure S2. Differentially expressed genes (DEGs) found between *B. oleracea* parents**
489 **used to generate a DH population.** a) Scatter plot showing the average expression of all
490 genes for A12DHd and GDDH33 (normalised DESeq2). Red dots indicate differentially
491 expressed genes. b) Heatmap of the 3,216 differentially expressed genes between A12DHd
492 and GDDH33 with hierarchal clustering. Scale shows log2 DESeq2 normalised expression.
493
494 **Figure S3. Heatmaps of parent-F1 hybrid differentially expressed genes (phDEGs).** a)
495 Heatmap of additive phDEGs. b) Heatmap of non-additively expressed phDEGs. Scale shows
496 log2 DESeq2 normalised expression.
497
498 **Figure S4. DNA methylation analysis in *B. oleracea* parents and F1 hybrids.** a) Histogram
499 displaying the frequency of cytosines with 0-100% methylation, the panel in each corner shows
500 the frequency of cytosines with 1-100% methylation. CG (top), CHG (middle), CHH (bottom).
501 b) Average methylation percentage across all cytosines. c) The average methylation across
502 chromosome 1 in bins of 1 Mb. d) and e) Average methylation across genes and transposons.
503 Within the feature body each feature is split into 100 bins and then each cytosine within this
504 bin is averaged for each feature in the genome.

505 **Figure S5. Numbers and genome distribution of differentially methylated regions in *B.**
506 ***oleracea* parents (pDMRs)**. a) Barplot of the numbers of DMRs between A12DHd and
507 GDDH33 in each sequence context. DMRs with higher methylation in A12DHd are shown in
508 yellow and DMRs with higher methylation in GDDH33 are shown in blue. b) Location of these
509 DMRs within genomic features, each base of a set of DMRs is assigned to the feature that it
510 overlaps with. Then the results are displayed as a percentage of the total bases in that set.
511 For each sequence context both A12DHd MRs and GDDH33 MRs are shown. Then the DMRs
512 between these two genotypes are split into DMRs with higher methylation in A12DHd (A12)
513 and DMRs with higher methylation in GDDH33 (GD). WG refers to the assignment of all the
514 bases in the reference genome when assigned to a feature. This is done in a hierarchical
515 fashion to account for overlapping features (gene, transposon, upstream, downstream,
516 intergenic: in order of decreasing importance)

517 **Figure S6. Heatmaps of differentially methylated regions found in *B. oleracea* parents-**
518 **F1 hybrid comparisons (phDMRs)**. Methylation of the F1 is most similar to A12DHd for

519 both additive and non-additive phDMRs. a) Additive phDMRs. b) Non-additive phDMRs. For
520 each sequence context; CG, CHG and CHH. Scale shows the methylation rate of the DMR.

521 **Figure S7. Schematic diagram describing how d/a ratios are calculated and plotted**. The
522 ratios are used to show how the dynamics of a DMR or gene in F1 hybrid relate to the parental
523 methylation or expression. a) The calculation of the ratios. Firstly, three pairwise comparisons
524 are performed (A12DHd - F1, GDDH33 - F1 and A12DHd - GDDH33). Then for each of these
525 genes or DMRs shown to be significant in at least one comparison, two ratios are calculated.
526 The d/a ratio and the parental d/a ratio. b) Displays the meaning of the ratios. The d/a ratio
527 (left histogram) describes the methylation of the DMR or expression of the gene in the F1
528 according to the high or low parent (parent with highest or lowest expression). The parental
529 d/a ratio (right histogram) describes the methylation of the DMR or expression of the gene in
530 the F1 according to the expression of the maternal parent (A12DHd) or the paternal parent
531 (GDDH33). The histograms show the thresholds imposed on these ratios that decide the
532 expression or methylation category (additive, parental-level dominance or above / below
533 parental levels. c) Plotting and display of the ratios and categories. In the top plot, each genes
534 ratios are plotted, the d/a ratio on the y-axis and the parental d/a ratio is plotted on the x-axis.
535 Plotting in this way, each differentially expressed feature can be categorised according to both
536 the high / low parent and the maternal / paternal parent. The bottom table of c) shows this
537 categorisation. Roman numerals show the categories as they are commonly described (Yoo
538 et al., 2013). Underneath the Roman numerals in the table, there is a graphic displaying the
539 expression or methylation pattern of this category for the 3 genotypes (A12DHd - maternal,
540 GDDH33 - paternal and F1)

541 **Figure S8. Schematic showing the process for HR site detection.** Top – SNP genotyping
542 method. Bottom – epi-genotyping method.
543
544 **Figure S9. Example of HR sites from line 2069.**

545 **Figure S10. Parental dominant-to-additive ratios of the dhDEGs.** For each inherited
546 genome dhDEGs tend to display expression dynamics similar to that of the other parental
547 genome. From left to right; Top - 2069, 3088, 3238, Middle - 1047, 5071, 1003, Bottom - 5119,
548 2134, 3013. For each line their A12DHd inherited dhDEGs are shown in yellow and the
549 GDDH33 inhertied dhDEGs are shown in blue. The x-axis displays the parental d/a ratio, a
550 ratio of 1 would mean a gene has equal expression to the gene in A12DHd and a ratio of -1
551 means the gene would have equal expression to the GDDH33 parent

Figure S11. Combined Gene Ontology analysis of dhDEGs. Each node represents an enriched GO term. (FDR <0.05). Size of node and label represents the number of DH lines a given term is enriched in.

Figure S12. Distribution of DNA methylation at transposable elements in *B. oleracea* double haploid lines. a) Distribution of methylation at transposable elements in the genome of double haploids compared to their parental origin (solid lanes). b) Differences in the distribution of DNA methylation at transposons for individual DH lines according to their genome. c) Differences in the distribution of DNA methylation at transposons for individual DH lines according to the type of transposon.

Figure S13. Distribution of dhDMR in different genomic features. Each DMR was assigned to a genomic feature and the proportion of bases for each category is displayed.

Figure S14. Genome-wide intersection between transcriptional and epigenetic variation in *B. oleracea* double haploid lines. Graphical representation of regions of the *B. oleracea* genome showing an overlap between transcriptional and DNA methylation variation in DH lines.

Figure S15. Additional examples of *B. oleracea* genes showing a direct correlation between transcriptional and epigenetic variation. a) Correlation between DNA methylation and expression in parents and DH lines at FAS-4 like locus (Bo9g121160). b) Correlation between DNA methylation and expression in parents and DH lines at Temperature-Induced Lipocalin locus (Bo9g134760). Left-hand side, single nucleotide resolution plot of methylation; Right-hand side shows normalised expression values.

References:

1. Blakeslee AF, Belling J, Farnham ME, Bergner AD: **A Haploid Mutant in the Jimson Weed, "Datura Stramonium".** *Science* 1922, **55:**646-647.
2. Kalinowska K, Chamas S, Unkel K, Demidov D, Lermontova I, Dresselhaus T, Kumlehn J, Dunemann F, Houben A: **State-of-the-art and novel developments of in vivo haploid technologies.** *Theor Appl Genet* 2019, **132:**593-605.
3. Guha S, Maheshwari SC: **In Vitro Production of Embryos from Anthers of Datura.** *Nature* 1964, **204:**497.
4. Ferrie AMR, Möllers C: **Haploids and doubled haploids in Brassica spp. for genetic and genomic research.** *Plant Cell Tiss Organ Cult* 2010, **104:**375-386.
5. Yan G, Liu H, Wang H, Lu Z, Wang Y, Mullan D, Hamblin J, Liu C: **Accelerated Generation of Selfed Pure Line Plants for Gene Identification and Crop Breeding.** *Front Plant Sci* 2017, **8:**1786.

6. Dunwell JM: **Haploids in flowering plants: origins and exploitation.** *Plant Biotechnol J* 2010, **8:**377-424.
7. Langridge P, Fleury D: **Making the most of 'omics' for crop breeding.** *Trends Biotechnol* 2011, **29:**33-40.
8. Chen ZJ: **Genomic and epigenetic insights into the molecular bases of heterosis.** *Nat Rev Genet* 2013, **14:**471-482.
9. Greaves IK, Eichten SR, Groszmann M, Wang A, Ying H, Peacock WJ, Dennis ES: **Twenty-four-nucleotide siRNAs produce heritable trans-chromosomal methylation in F1 Arabidopsis hybrids.** *Proc Natl Acad Sci U S A* 2016, **113:**E6895-E6902.
10. Groszmann M, Gonzalez-Bayon R, Lyons RL, Greaves IK, Kazan K, Peacock WJ, Dennis ES: **Hormone-regulated defense and stress response networks contribute to heterosis in Arabidopsis F1 hybrids.** *Proc Natl Acad Sci U S A* 2015, **112:**E6397-6406.
11. Kirkbride RC, Yu HH, Nah G, Zhang C, Shi X, Chen ZJ: **An Epigenetic Role for Disrupted Paternal Gene Expression in Postzygotic Seed Abortion in Arabidopsis Interspecific Hybrids.** *Mol Plant* 2015, **8:**1766-1775.
12. Koussounadis A, Langdon SP, Um IH, Harrison DJ, Smith VA: **Relationship between differentially expressed mRNA and mRNA-protein correlations in a xenograft model system.** *Sci Rep* 2015, **5:**10775.
13. Rigal M, Becker C, Pelissier T, Pogorelcnik R, Devos J, Ikeda Y, Weigel D, Mathieu O: **Epigenome confrontation triggers immediate reprogramming of DNA methylation and transposon silencing in Arabidopsis thaliana F1 epihybrids.** *Proc Natl Acad Sci U S A* 2016, **113:**E2083-2092.
14. Zhang Q, Wang D, Lang Z, He L, Yang L, Zeng L, Li Y, Zhao C, Huang H, Zhang H, et al: **Methylation interactions in Arabidopsis hybrids require RNA-directed DNA methylation and are influenced by genetic variation.** *Proc Natl Acad Sci U S A* 2016, **113:**E4248-4256.
15. De Block M, Van Lijsebettens M: **Energy efficiency and energy homeostasis as genetic and epigenetic components of plant performance and crop productivity.** *Curr Opin Plant Biol* 2011, **14:**275-282.
16. Hauben M, Haesendonckx B, Standaert E, Van Der Kelen K, Azmi A, Akpo H, Van Breusegem F, Guisez Y, Bots M, Lambert B, et al: **Energy use efficiency is characterized by an epigenetic component that can be directed through artificial selection to increase yield.** *Proc Natl Acad Sci U S A* 2009, **106:**20109-20114.
17. Verkest A, Byzova M, Martens C, Willems P, Verwulgen T, Slabbinck B, Rombaut D, Van de Velde J, Vandepoele K, Standaert E, et al: **Selection for Improved Energy Use Efficiency and Drought Tolerance in Canola Results in Distinct Transcriptome and Epigenome Changes.** *Plant Physiol* 2015, **168:**1338-1350.
18. Blary A, Gonzalo A, Eber F, Berard A, Berges H, Bessoltane N, Charif D, Charpentier C, Cromer L, Fourment J, et al: **FANCM Limits Meiotic Crossovers in Brassica Crops.** *Front Plant Sci* 2018, **9:**368.
19. Pele A, Falque M, Trotoux G, Eber F, Negre S, Gilet M, Huteau V, Lode M, Jousseaume T, Dechaumet S, et al: **Amplifying recombination genome-wide and reshaping crossover landscapes in Brassicas.** *PLoS Genet* 2017, **13:**e1006794.
20. Swanson-Wagner RA, Jia Y, DeCook R, Borsuk LA, Nettleton D, Schnable PS: **All possible modes of gene action are observed in a global comparison of gene expression in a maize F1 hybrid and its inbred parents.** *Proc Natl Acad Sci U S A* 2006, **103:**6805-6810.
21. Yoo MJ, Szadkowski E, Wendel JF: **Homoeolog expression bias and expression level dominance in allopolyploid cotton.** *Heredity (Edinb)* 2013, **110:**171-180.
22. Hu X, Wang H, Diao X, Liu Z, Li K, Wu Y, Liang Q, Wang H, Huang C: **Transcriptome profiling and comparison of maize ear heterosis during the spikelet and floret differentiation stages.** *BMC Genomics* 2016, **17:**959.

23. Kawanabe T, Ishikura S, Miyaji N, Sasaki T, Wu LM, Itabashi E, Takada S, Shimizu M, Takasaki-Yasuda T, Osabe K, et al: **Role of DNA methylation in hybrid vigor in Arabidopsis thaliana.** *Proc Natl Acad Sci U S A* 2016, **113:**E6704-E6711.
24. Hegarty MJ, Barker GL, Wilson ID, Abbott RJ, Edwards KJ, Hiscock SJ: **Transcriptome shock after interspecific hybridization in senecio is ameliorated by genome duplication.** *Curr Biol* 2006, **16:**1652-1659.
25. Otto SP: **The evolutionary consequences of polyploidy.** *Cell* 2007, **131:**452-462.
26. Song Q, Chen ZJ: **Epigenetic and developmental regulation in plant polyploids.** *Curr Opin Plant Biol* 2015, **24:**101-109.
27. Bottani S, Zabet NR, Wendel JF, Veitia RA: **Gene Expression Dominance in Allopolyploids: Hypotheses and Models.** *Trends Plant Sci* 2018, **23:**393-402.
28. Veitia RA, Bottani S, Birchler JA: **Gene dosage effects: nonlinearities, genetic interactions, and dosage compensation.** *Trends Genet* 2013, **29:**385-393.
29. Law JA, Ausin I, Johnson LM, Vashisht AA, Zhu JK, Wohlschlegel JA, Jacobsen SE: **A protein complex required for polymerase V transcripts and RNA- directed DNA methylation in Arabidopsis.** *Curr Biol* 2010, **20:**951-956.
30. Heslop-Harrison JS: **Gene expression and parental dominance in hybrid plants.** *Dev Suppl* 1990**:**21-28.
31. Kruglova AA, Matveeva NM, Gridina MM, Battulin NR, Karpov A, Kiseleva EV, Morozova KN, Serov OL: **Dominance of parental genomes in embryonic stem cell/fibroblast hybrid cells depends on the ploidy of the somatic partner.** *Cell Tissue Res* 2010, **340:**437-450.
32. Matveeva NM, Fishman VS, Zakharova IS, Shevchenko AI, Pristyazhnyuk IE, Menzorov AG, Serov OL: **Alternative dominance of the parental genomes in hybrid cells generated through the fusion of mouse embryonic stem cells with fibroblasts.** *Sci Rep* 2017, **7:**18094.
33. Birchler JA, Yao H, Chudalayandi S: **Unraveling the genetic basis of hybrid vigor.** *Proc Natl Acad Sci U S A* 2006, **103:**12957-12958.
34. Govindaraju DR: **An elucidation of over a century old enigma in genetics-Heterosis.** *PLoS Biol* 2019, **17:**e3000215.
35. Crossa J, Perez-Rodriguez P, Cuevas J, Montesinos-Lopez O, Jarquin D, de Los Campos G, Burgueno J, Gonzalez-Camacho JM, Perez-Elizalde S, Beyene Y, et al: **Genomic Selection in Plant Breeding: Methods, Models, and Perspectives.** *Trends Plant Sci* 2017, **22:**961-975.
36. Bohuon EJ, Keith DJ, Parkin IA, Sharpe AG, Lydiate DJ: **Alignment of the conserved C genomes of Brassica oleracea and Brassica napus.** *Theor Appl Genet* 1996, **93:**833-839.
37. Andrews S: **FastQC: A quality control tool for high-throughput sequence data.** 2010.
38. Bolger AM, Lohse M, Usadel B: **Trimmomatic: a flexible trimmer for Illumina sequence data.** *Bioinformatics* 2014, **30:**2114-2120.
39. Parkin IA, Koh C, Tang H, Robinson SJ, Kagale S, Clarke WE, Town CD, Nixon J, Krishnakumar V, Bidwell SL, et al: **Transcriptome and methylome profiling reveals relics of genome dominance in the mesopolyploid Brassica oleracea.** *Genome Biol* 2014, **15:**R77.
40. Trapnell C, Hendrickson DG, Sauvageau M, Goff L, Rinn JL, Pachter L: **Differential analysis of gene regulation at transcript resolution with RNA-seq.** *Nat Biotechnol* 2013, **31:**46-53.
41. Anders S, Pyl PT, Huber W: **HTSeq--a Python framework to work with high-throughput sequencing data.** *Bioinformatics* 2015, **31:**166-169.
42. Love MI, Huber W, Anders S: **Moderated estimation of fold change and dispersion for RNA-seq data with DESeq2.** *Genome Biol* 2014, **15:**550.
43. Krueger F, Andrews SR: **Bismark: a flexible aligner and methylation caller for Bisulfite-Seq applications.** *Bioinformatics* 2011, **27:**1571-1572.

44. Catoni M, Tsang JM, Greco AP, Zabet NR: **DMRcaller: a versatile R/Bioconductor package for detection and visualization of differentially methylated regions in CpG and non-CpG contexts.** *Nucleic Acids Res* 2018, **46:**e114.
45. Guo T, Li H, Yan J, Tang J, Li J, Zhang Z, Zhang L, Wang J: **Performance prediction of F1 hybrids between recombinant inbred lines derived from two elite maize inbred lines.** *Theor Appl Genet* 2013, **126:**189-201.
46. Barturen G, Rueda A, Oliver JL, Hackenberg M: **MethylExtract: High-Quality methylation maps and SNV calling from whole genome bisulfite sequencing data.** *F1000Res* 2013, **2:**217.
47. Hofmeister BT, Lee K, Rohr NA, Hall DW, Schmitz RJ: **Stable inheritance of DNA methylation allows creation of epigenotype maps and the study of epiallele inheritance patterns in the absence of genetic variation.** *Genome Biol* 2017, **18:**155.
48. Yoo SD, Cho YH, Sheen J: **Arabidopsis mesophyll protoplasts: a versatile cell system for transient gene expression analysis.** *Nat Protoc* 2007, **2:**1565-1572.

Figure 1

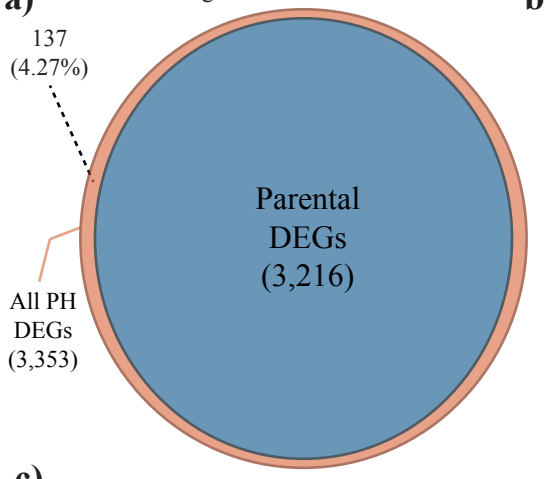

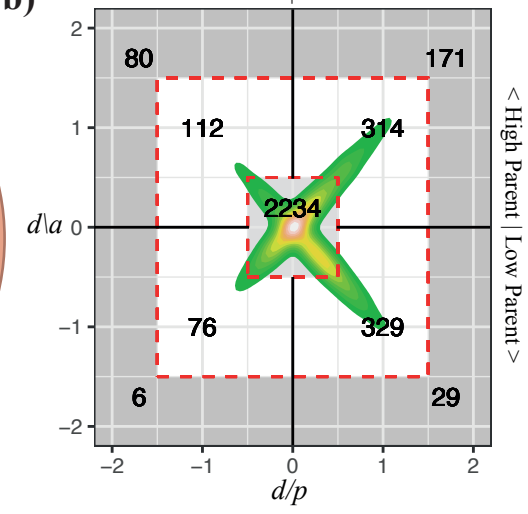

c)

Additivity		GDDH33DHL expression level dominance		A12Ddh expression level dominance		Transgressive down-regulation			Transgressive up-regulation		
I	XII	II	XI	IV	IX	III	VII	X	V	VI	VIII
♀ F1 ♂	♀ F1 ♂	♀ F1 ♂	♀ F1 ♂	♀ F1 ♂	♀" F1♂	♀ F1 ♂	♀ F1 ♂	♀ F1 ♂	♀ F1 ♂	♀ F1 ♂	♀ F1 ♂
66.6%		3.3%	2.3%	9.4%	9.8%	1.0%			7.5%		

Figure 2

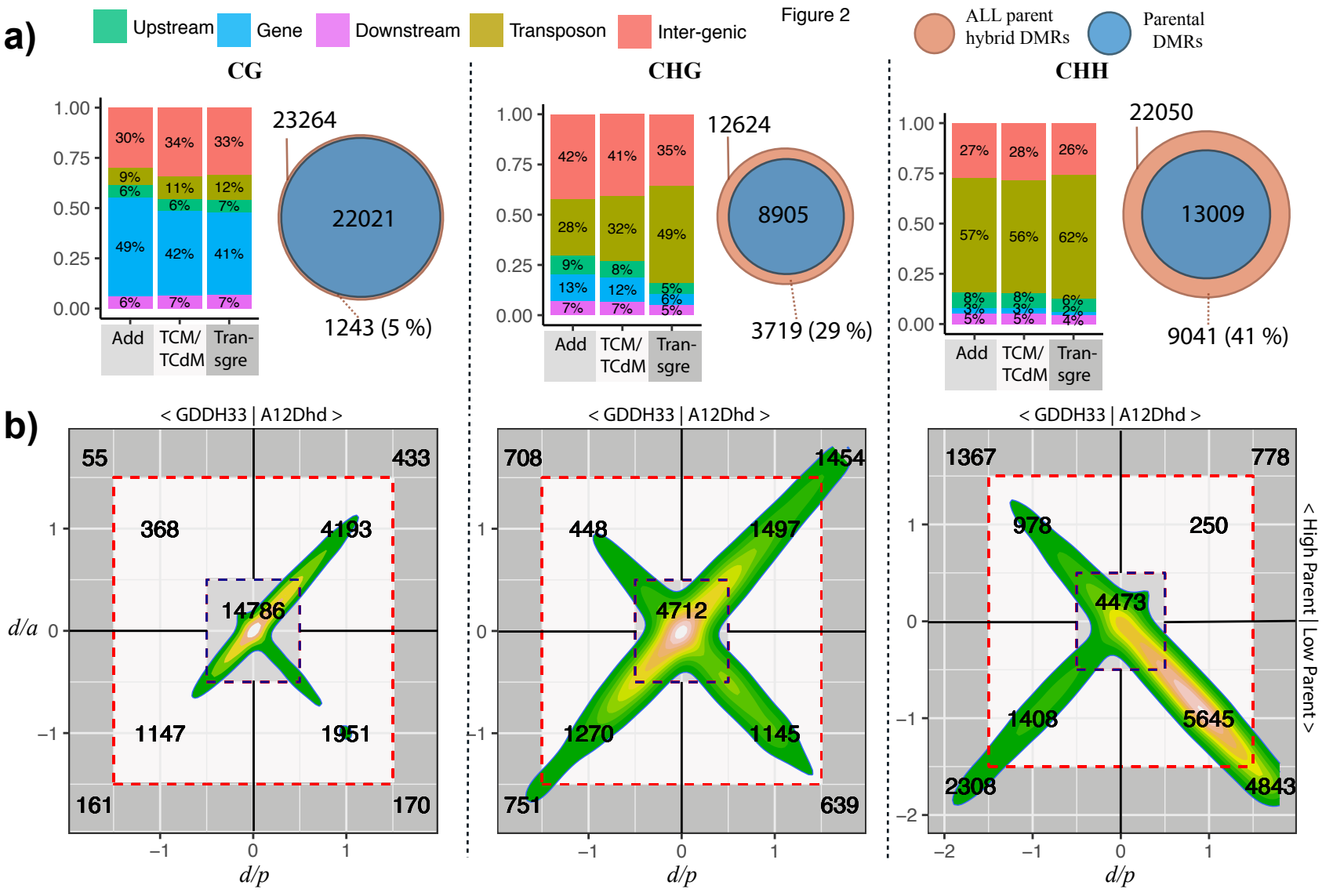

	Additivity		GDDH33 Level TCM / TCdM		A12DHL Level TCM / TCdM		Transgressive de-methylation			Transgressive methylation		
	I	XII	II	XI	IV	IX	III	VII	X	V	VI	VIII
	♀ F1 ♂	♀ F1 ♂	♀ F1 ♂	♀ F1 ♂	♀ F1 ♂	♀ F1 ♂	♀ F1 ♂	♀ F1 ♂	♀ F1 ♂	♀ F1 ♂	♀ F1 ♂	♀ F1 ♂
CG	63.5%		1.5%	4.9%	18.0%	8.3%	1.4%			2.0%		
CHG	37.3%		3.5%	10.0%	11.9%	9.1%	11.0%			17.1%		
CHH	20.3%		4.4%	6.4%	1.1%	25.6%	32.4%			9.7%		

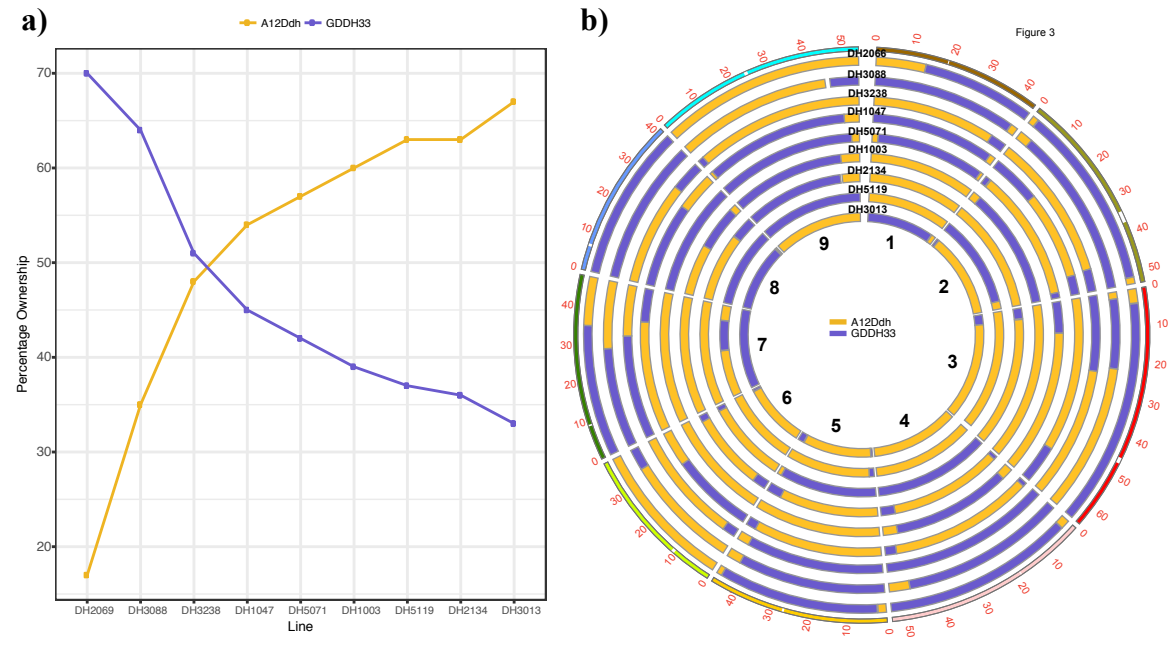
a)
A12Ddh
GDDH33
Percentage Ownership
70
60
50
40
30
20
DH2069
DH3088
DH3238
DH1047
DH5071
DH1003
DH5119
DH2134
DH3013
Line
b)
Figure 3
DH2066
DH3088
DH3238
DH1047
DH5071
DH1003
DH2134
DH5119
DH3013
1
2
3
4
5
6
7
8
9
A12Ddh
GDDH33

Figure 4

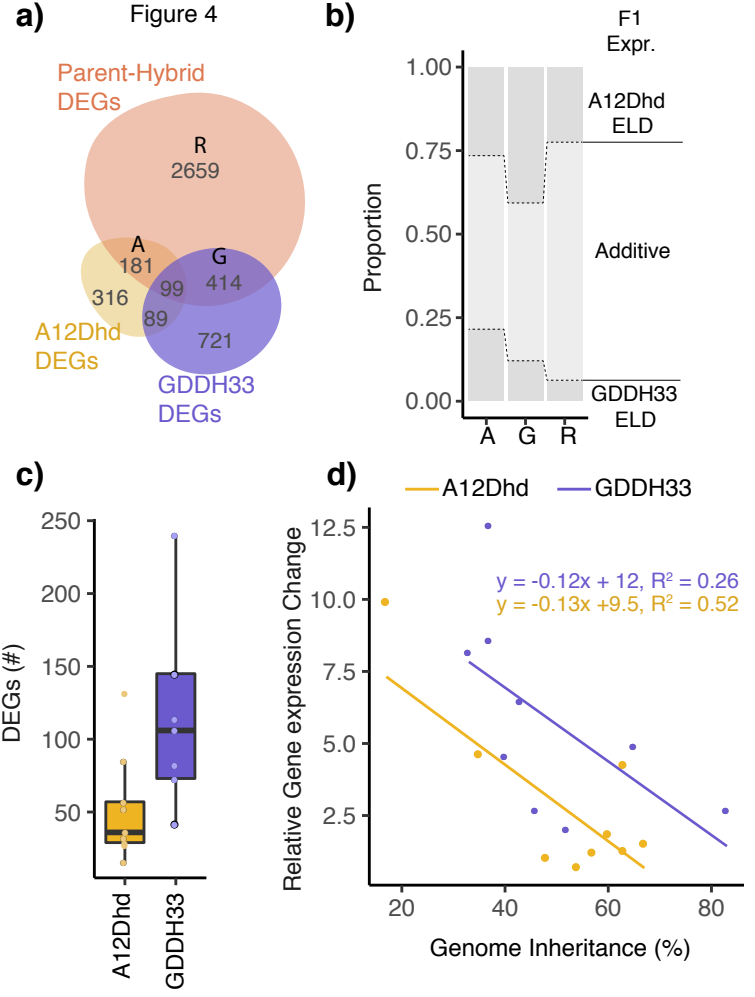
a)
Parent-Hybrid DEGs
R
2659
A
181
G
414
316
99
89
721
A12Dhd DEGs
GDDH33 DEGs
b)
F1 Expr.
1.00
0.75
0.50
0.25
0.00
Proportion
A12Dhd ELD
Additive
GDDH33 ELD
A
G
R
c)
250
200
150
100
50
DEGs (#)
A12Dhd
GDDH33
d)
A12Dhd
GDDH33
y = -0.12x + 12, R² = 0.26
y = -0.13x +9.5, R² = 0.52
12.5
10.0
7.5
5.0
2.5
Relative Gene expression Change
20
40
60
80
Genome Inheritance (%)

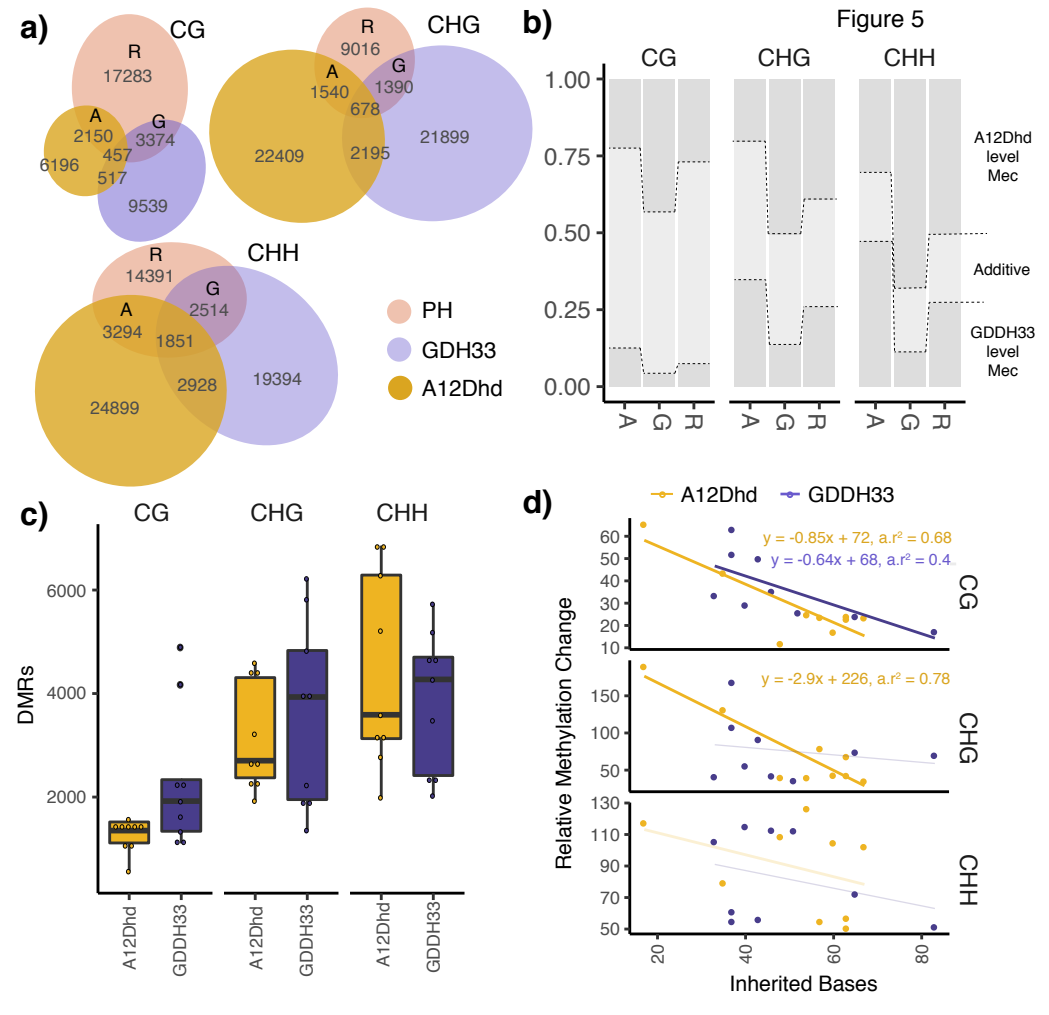
a)
CG
R
17283
A
2150
G
3374
457
6196
517
9539
CHG
R
9016
A
1540
G
1390
678
22409
2195
21899
CHH
R
14391
G
2514
A
3294
1851
2928
19394
24899
PH
GDH33
A12Dhd
b)
Figure 5
CG
CHG
CHH
1.00
0.75
0.50
0.25
0.00
A12Dhd level Mec
Additive
GDDH33 level Mec
A
G
R
c)
CG
CHG
CHH
DMRs
6000
4000
2000
A12Dhd
GDDH33
d)
A12Dhd
GDDH33
y = -0.85x + 72, a.r² = 0.68
y = -0.64x + 68, a.r² = 0.4
y = -2.9x + 226, a.r² = 0.78
Relative Methylation Change
Inherited Bases
20
40
60
80

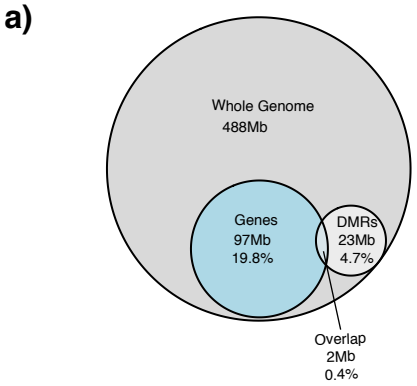
a)
Whole Genome
488Mb
Genes
97Mb
19.8%
DMRs
23Mb
4.7%
Overlap
2Mb
0.4%

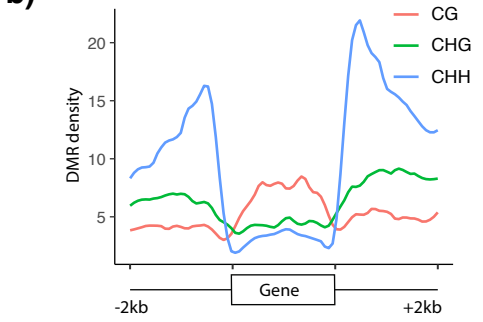
b)
CG
CHG
CHH
DMR density
20
15
10
5
Gene
-2kb
+2kb

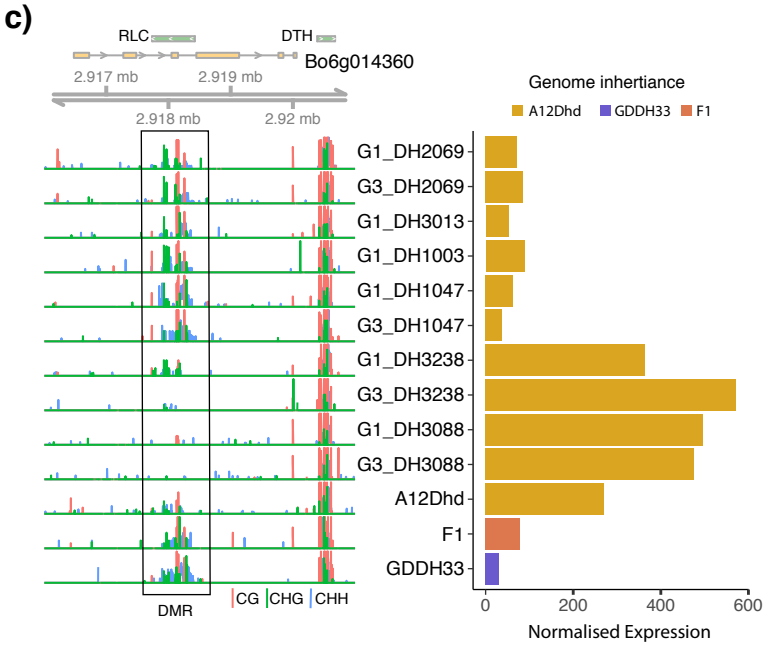
c)
RLC
DTH
Bo6g014360
2.917 mb
2.919 mb
2.918 mb
2.92 mb
DMR
CG
CHG
CHH
Genome inheritance
A12Dhd
GDDH33
F1
G1_DH2069
G3_DH2069
G1_DH3013
G1_DH1003
G1_DH1047
G3_DH1047
G1_DH3238
G3_DH3238
G1_DH3088
G3_DH3088
A12Dhd
F1
GDDH33
0
200
400
600
Normalised Expression

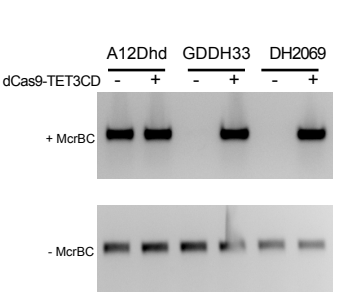
d)
A12Dhd
GDDH33
DH2069
dCas9-TET3CD
-
+
-
+
-
+
+ McrBC
- McrBC

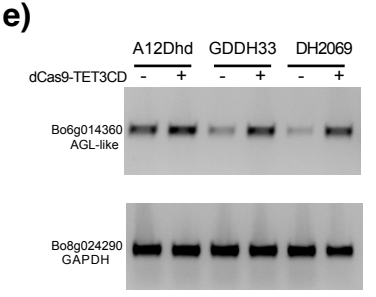
e)
A12Dhd
GDDH33
DH2069
dCas9-TET3CD
-
+
-
+
-
+
Bo6g014360
AGL-like
Bo8g024290
GAPDH